(14) Matsuda, H.; Yamano, K.; Inagaki, H. *J. Polym. Sci., Part A-2* **1969**, *7*, 609.
(15) Flory, J. P. *Statistical Mechanics of Chain Molecules*; Interscience: New York, 1969; Chapter II.
(16) Anufrieva, E. V.; Gotlib, Yu. Ya. *Adv. Polym. Sci.* **1981**, *40*, 1.
(17) Zind, M.; Edsall, J. T. *J. Am. Chem. Soc.* **1937**, *59*, 2247.
(18) Chen, H.-L.; Morawetz, H. *Eur. Polym. J.* **1983**, *19*, 923. Turro, N. J.; Arora, K. S. *Polymer* **1986**, *27*, 783. Studies of the analogous complexation of PMA with PVP have been reported by: Papisov, I. M.; Baranovskii, V. Yu.; Kabanov, V. A. *Vysokomol. Soed.* **1975**, *A16*, 2104; and by Osada, Y. *J. Polym. Sci., Polym. Chem. Ed.* **1979**, *17*, 3485.

Photophysical and Photochemical Studies on a Polymeric Intramolecular Micellar System, PA-18K_2

Deh-Ying Chu and J. K. Thomas*

Department of Chemistry, University of Notre Dame, Notre Dame, Indiana 46556.
Received February 17, 1987

ABSTRACT: A polymeric intramolecular micellar system, PA-18K_2 which is a potassium salt of a 1:1 copolymer of maleic anhydride and 1-octadecene, has been investigated via steady-state emission, absorption, time-dependent emission and transient absorption spectroscopy, etc. Pyrene and some of its positively charged derivatives and negatively charged derivatives can be solubilized in the interior of PA-18K_2 over the entire pH range. It is observed that there is a significant effect of the polymer main chain surrounding the polymer micelles on the bimolecular quenching kinetics and exciplex formation of guest molecules. Both steady-state and pulsed studies indicate that guest molecules in PA-18K_2 experience a larger hydrophobicity than in sodium dodecyl sulfate micelles, but one that is similar to that in sodium cetyl sulfate micelles. Data from Poisson quenching kinetics suggest that one polymer micelle consists of about 25 monomer units; i.e., one PA-18K_2 polymer molecule of molecular weight 1×10^4 forms one polymer micelle.

Introduction

In the last few decades marked progress has been made in photophysical and photochemical studies in organized assemblies, which act as host systems for many hydrophobic molecules. A great variety of experimental data have been reported,[1-4] especially for simple micellar systems, which are aggregated structures formed by the interaction of several surfactant molecules, i.e., intermolecular micelles.

Polyelectrolytes with hydrophobic side chains may exhibit behavior reminiscent of micelles under appropriate conditions. The hydrophobic bonding between the paraffinic side chains in these systems results in stabilization of compact structures, analogous to micelles. Such polymers have been called "polysoaps" or intramolecular micelle-forming polymers. Typical examples are the *n*-dodecyl derivatives of poly(4-vinylpyridine),[5] poly(vinylbenzo-18-crown-6).[6] Synthetic weak polyelectrolytes such as poly(methacrylic acid), PMA,[7] and copolymers of maleic anhydride and *n*-alkylvinyl ethers (n = 4–8)[8] are known to provide hydrophobic microdomains in the low pH range; i.e., compact polymer coils are only formed in strongly acidic solution, while the compact conformation is converted into the extended rod or coil form at high pH. For any practical use of the polymer as a host material for hydrophobic molecules, strongly acidic polymers should be avoided, and a hydrophobic environment is required close to neutral pH. Polyelectrolytes with longer hydrocarbon side chains are expected to behave as hypercoils over the entire pH range. PA-18K_2, which is a potassium salt of an alternating copolymer of maleic anhydride and 1-octadecene, offers such an example.

Reports concerning photophysical and photochemical studies in "polysoap" systems are infrequent and mainly focus on steady-state studies.[9,10] In the present paper, PA-18K_2 has been investigated by steady-state and pulsed studies. The results are compared to previous studies in PMA systems[11,16] in order to ascertain the effect of long hydrocarbon side chains on the formation of intramolecular micelles.[11c] The comparison of polymer micelle and simple micellar systems was also made in order to study the effect of the polymer main chain on the quenching kinetics of pyrene and pyrene derivatives in these systems. Finally, Poisson quenching kinetics to estimate the mean aggregation number of monomer units and double-exponential kinetics to estimate the equilibrium constant of pyrene between the aqueous phase and polymer micelle are presented.

Experimental Section

Polymer Materials. PA-18, a copolymer derived from 1-octadecene and maleic anhydride, was supplied by Chevron/Gulf Co. The molar ratio of comonomers is referred to as 1:1. PA-18 has a molecular weight of about 1×10^4, measured by HPLC with an ultrastyragel permeation column calibrated with standard samples of polystyrenes. The potassium salt of PA-18, PA-18K_2 was prepared by adding 45 g PA-18 (0.1 mol), while stirring, to 50 g of 30% KOH solution (0.24 mol) heated above 85 °C; after

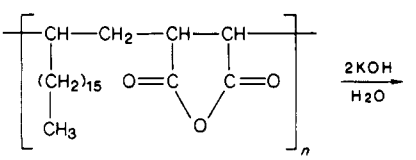

PA-18

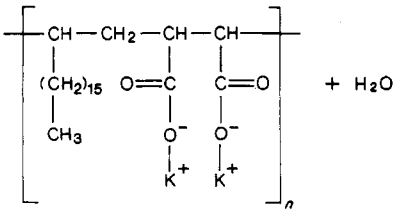

PA-18K_2

all solids dissolved, 150 mL of water was added. The salt PA-18K_2 was precipated by addition of a 2-fold excess of methanol to the filtered solution, washed with methanol, reprecipitated from hot water twice, and finally vacuum-dried at 40 °C. IR spectra showed that hydrolysis of the starting material was complete; i.e., the

0024-9297/87/2220-2133$01.50/0

stretching bands of C=O (1780 and 1850 cm^{-1}) completely shifted to lower frequencies (1410 and 1580 cm^{-1}) due to the release of anhydride ring strain, while the stretching bands of C—O showed similar shifts. The concentrations of polymer solutions used in the present work are expressed as polymer chain units. The concentration of PA-18K_2 samples is 1×10^{-4} M unless stated otherwise.

Fluorescent Probes and Quenchers. The fluorescent probes used are pyrene, 1-pyrenebutyltrimethylammonium bromide (C_4PN^+), 1-pyreneundecyltrimethylammonium iodide ($C_{11}PN^+$), 1-pyrenebutyric acid (PyC_3COOH), 1-pyrenedecanoic acid (PyC_9COOH), 1-pyrenesulfonic acid sodium salt ($PySO_3Na$), and 2-methylanthracene.[11]

Quenchers used are sodium iodide and thallium(I) sulfate which were used as received. However, nitromethane (CH_3NO_2) and dimethylaniline (DMA) were purified by vacuum distillation; 1-dodecylpyridinium chloride (DPC) was purified by double recrystallization from absolute ethanol.

Surfactants. Sodium dodecyl sulfate, SDS (BHD Chem.) and sodium cetyl sulfate, SCS (Research plus Lab.) were used as received. SDS was chosen as a simple micellar system for comparison at room temperature, while SCS, due to its low solubility in water at room temperature, was used at 40 °C. The concentrations of surfactants used in the present studies are 5×10^{-2} (SDS) and 2×10^{-3} M (SCS).

Sample Preparation and Measurements. The concentrated PA-18K_2 solution, 1×10^{-3} M, was prepared by heating above 70 °C and then cooling to room temperature. This solution was stored and was stable for over a month. The pH of the sample was adjusted with concentrated HCl or NaOH aqueous solution and measured with a Sargent-Welch combination electrode at 20 °C; by using a model LS pH meter; the pH meter was calibrated with standard buffer solutions of pH 4, 7, and 10. For most studies, PA-18K_2 samples were adjusted to pH 8, i.e., close to conditions for practical use.

Steady-state absorption spectra and emission spectra were recorded on a Perkin-Elmer 552 UV–visible and MPF-44B fluorescence spectrophotometers, respectively. The ratio I_3/I_1 is the ratio of the intensity of the pyrene monomer fluorescence intensity of peak 3 (λ 384 nm) to peak 1 (λ 373 nm), which was used to monitor probe environment. The measurements of the degree of polarization,[12] decay rate constants, quenching rate constants, and transient absorption have been described in previous studies.[13]

Results and Discussion

Hydrophobic Microdomains in PA-18K_2. Previous studies show that the ratio of the pyrene fluorescence intensitites of peak 3 to peak 1 can be used to monitor the environment of excited pyrene and higher values of I_3/I_1, indicating a more hydrophobic environment for pyrene.[14]

Figure 1 shows the effect of pH on the fluorescence intensity ratio, I_3/I_1, of pyrene in aqueous solutions of PA-18K_2 and PMA. In the case of PA-18K_2, the ratio of I_3/I_1 is almost constant and remains at 1.09–1.04 over the entire range. These data contrast with those observed in aqueous solutions of PMA where the ratio I_3/I_1 sharply decreases from 0.88 to 0.55 at pH > 4. The data indicate that PMA acts as a host for pyrene only in the low pH range. However, the PA-18K_2 provides hydrophobic microdomains and acts as a host over the entire pH range. Increasing pH increases the ionization of the polymers which leads to a repulsive interaction of negatively charged carboxy (COO^-) groups and tends to expand the polymer; in the PA-18K_2 system, a strong hydrophobic interaction exists among the long hydrocarbon side chains which stabilizes the compact conformations even at high pH. It is expected that if methyl groups of PMA are replaced by longer chains a hypercoil will be formed both at low pH and high pH as in the PA-18K_2 system.

The fluorescence decay rate constants, k_0, of several fluorescent probes in various systems are summarized in Table I and provide further evidence about the hydrophobic microdomains in PA-18K_2 aqueous solutions. All the k_0's at pH 4, 8, and 10 are close or similar to those found in hexanol and much smaller than those in water. One exception is $PySO_3Na$, which is not solubilized in PA-18K_2 at either pH 4 or pH 8 or pH 10. It is also noted that the decay of PyC_3COOH increases with increasing pH and approaches that in water. The behavior of PyC_3COOH, unlike pyrene, is explained by the ionization of PyC_3COOH, giving the PyC_3COO^- anion, which leads to ejection of the ionized probe by the negatively charged polymer surface at high pH. However, the data for longer chain PyC_9COOH do not exhibit a significant change in decay rate with pH. It is suggested that the polymer micelle hosts the probe PyC_9COOH at both pH 4 and at higher pH due to the hydrophobic interaction between the hydrocarbon chains of PA-18K_2 and the longer PyC_9COOH chains which locate the molecule in the micelle. On the other hand, the decay of the positively charged probe C_4PN^+ decreases with increasing pH and is close to that in hexanol. The faster decay of C_4PN^+ fluorescence at pH 4 is also explained by the low ionization of PA-18K_2 at pH 4, leading to less electrostatic binding between C_4PN^+ and polymer, which partially ejects C_4PN^+ from the polymer. Meanwhile long-chain $C_{11}PN^+$ exhibits identical decay rates over the entire pH range and can be explained by similar reasoning to the case of PyC_9COOH. In summary, PA-18K_2 readily solubilizes pyrene and some positively and negatively charged derivatives of pyrene, especially long-chain derivatives.

Pyrene fluorescence decay curves in PA-18K_2 at pH 8, in SDS and in water, are shown in Figure 2. It can be seen that the lifetime of the excited singlet pyrene in PA-18K_2 is much longer than in water and also longer than in SDS. The fluorescence spectroscopy data show that the ratio I_3/I_1 of pyrene fluorescence in PA-18K_2 (1.08) is much larger than in water (0.55) and even larger than in SDS (0.82). However, it is found that I_3/I_1 (0.95) and the

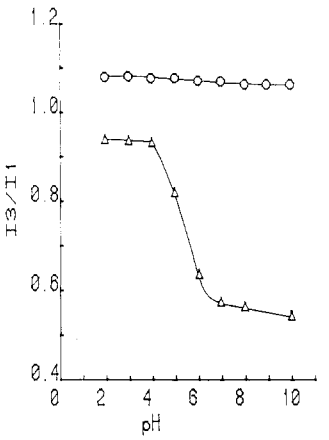

Figure 1. Relationship between the intensity ratio, I_3/I_1, of pyrene fluorescence and pH in aqueous solutions of PA-18K_2 (○) and PMA (△): [pyrene] = 2×10^{-6} M.

Table I
Decay Rate Constants of Fluorescence of Several Fluorescent Probes

	k_0, 10^7 s^{-1}				
	PA-18K_2				
probe	pH 4	pH 8	pH 10	hexanol	water
$PySO_3Na$	1.57	1.56	1.57	0.71	1.60
PyC_3COOH	0.42	0.74	0.79	0.45	0.80
PyC_9COOH	0.45	0.46	0.49	0.43	0.87
Pyrene	0.25	0.25	0.24	0.25	0.49
C_4PN^+	0.56	0.44	0.44	0.44	0.70
$C_{11}PN^+$	0.47	0.47	0.48	0.53	0.78

Table II
Quenching Rate Constants of Pyrene Fluorescence in Various Systems[a]

quenchers	k_q, M^{-1} s^{-1}			
	PA-18K$_2$ (pH 8)	SDS	heptane	water
none	2.5×10^6 s^{-1}	2.9×10^6 s^{-1}	2.2×10^6 s^{-1}	4.8×10^6 s^{-1}
Tl^+	7.6×10^{10}	2.6×10^{10}		6.2×10^9
O_2	3.2×10^9	9.2×10^9	5.5×10^{10}	9.8×10^9
CH_3NO_2	1.2×10^8	3.0×10^9	1.7×10^9	9.5×10^9
I^-	$< 10^6$	2.6×10^6		1.3×10^9

[a] [Pyrene] = 2×10^{-6} M.

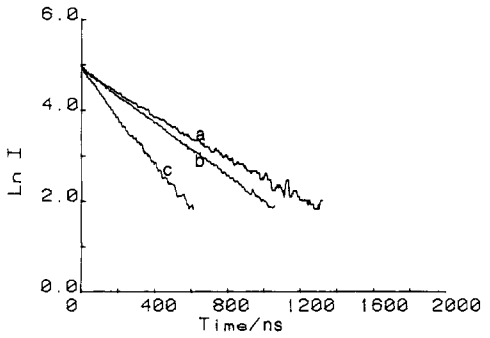

Figure 2. Decay curves of pyrene fluorescence, ln I, vs. time in aqueous solutions of PA-18K$_2$ (a), in SDS (b), and in water (c): [pyrene] = 2×10^6 M.

lifetime (~300 ns) of pyrene fluorescence in PA-18K$_2$ at 40 °C are similar to those observed in SCS micellar aqueous solutions, where the hydrocarbon chain length is identical with the side chains of PA-18K$_2$. The above data indicate that the interior of the polymeric PA-18K$_2$ micelle has a hydrophobicity larger than that of SDS. The hydrophobicity of PA-18K$_2$ is similar to that of SCS, yet PA-18K$_2$ has an advantage in that it can be used at room temperature under conditions when SCS precipitates.

Biomolecular Quenching Kinetics. The bimolecular quenching rate constants, k_q, of pyrene fluorescence in various systems are presented in Table II. The values of k_q with the quenchers such as oxygen, nitromethane, and sodium iodide in PA-18K$_2$ polymer micellar solutions are much smaller than in water or in homogeneous nonpolar solvents, viz. heptane, and even smaller than in SDS micellar solutions. The data suggest that the penetration of the selected quenchers to the pyrene hosted in the polymer micelle is inhibited by the main chain of the host polymer micelle. This restrictive effect is larger than in simple micellar systems and reflects on the more rigid environment of pyrene in polymer micellar systems. It is also noted that the k_q with iodide ion in the SDS micellar system is 10^3-fold smaller than in water due to the electrostatic repulsive interaction between the negatively charged micellar surface and the negatively charged quencher molecules. Nevertheless, in the iodide system, the electrostatic effect is smaller in PA-18K$_2$ than in SDS. The restrictive effect with nitromethane is larger than with oxygen and corresponds to previous studies,[11] indicating that O_2 tends to penetrate into the polymer micelle to a greater extent than CH_3NO_2. The negatively charged surfaces of polymer micelles or of simple micelles lead to binding of cations such as thallium ions to these surfaces, and the k_q values in micelles are larger than in water. The percentage of binding of thallium ions to micelles was obtained by measuring the quenching rate constants of 1-pyrenesulfonic acid sodium salt ($PySO_3Na$) by thallium sulfate in water and in micellar solution.[10a,15] It is found that binding of Tl^+ in PA-18K$_2$ (~80%) is more efficient than in SDS (~20%), resulting in more efficient quenching of pyrene fluorescence in PA-18K$_2$ than in SDS.

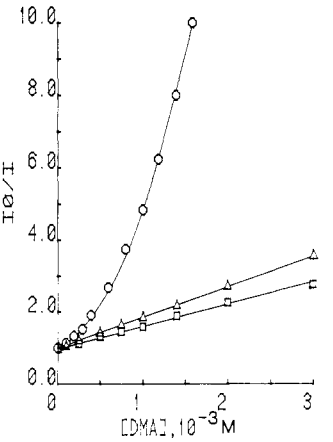

Figure 3. Stern–Volmer plot of pyrene fluorescence, I_0/I, vs. [DMA] in SDS (○), in PA-18K$_2$ (△), and in heptane (□): [pyrene] = 6×10^{-5} M, [DMA] = 0–3 mM.

The degree of polarization of 2-methylanthracene, P, was measured in various systems in order to gain more information about the rigidity of probe environment in these systems. The data show that P in PA-18K$_2$ at pH 8 (~0.14) is much larger than that in SDS (~0.01) but slightly less than that observed in PMA at pH 2 (~0.17). This illustrates that 2-methylanthracene in PA-18K$_2$ micelles experiences a much more rigid environment than in SDS but somewhat less than that in PMA compact coil at pH 2. The data are in correspondence with the above bimolecular quenching data and the results of previous studies.[16]

Pyrene–DMA Exciplex. Previous studies show that the quenching of pyrene fluorescence by dimethylaniline, DMA, is via an exciplex process. Figure 3 shows the plot of the pyrene monomer fluorescence intensity ratio I_0/I vs. [DMA] in aqueous solutions of SDS and PA-18K$_2$. Nonlinear rapid quenching behavior is observed at higher concentrations of DMA in SDS solutions and is explained in previous studies as an association of DMA with SDS micelles.[17] However, in polymer micelle solutions, the plot is linear; i.e., the data follow normal Stern–Volmer kinetics. The k_q in PA-18K$_2$ (2.1×10^9 M^{-1} s^{-1}) is similar to that found in heptane (1.9×10^9 M^{-1} s^{-1}), indicating that the quenching in PA-18K$_2$ is close to diffusion controlled and is linear over all DMA concentrations used. The data are best explained by the inhibition placed by the polymer main chain on the penetration of DMA into the micelle either at low or at high DMA concentrations. There is no static quenching at high DMA concentrations quite unlike the SDS micellar systems.

The transient absorption spectra of pyrene and DMA in the flash photolysis of aqueous solutions of PA-18K$_2$ and SDS are displayed in Figure 4. Previous studies[18] show that the quantum yield of excited triplet pyrene (ϕ_T) and the quantum yield of anion pyrene (ϕ_-) can be calculated from the optical densities of the transient absorption spectrum, using extinction coefficients $\epsilon(P_T^*) = 3.5 \times 10^4$ M^{-1} cm^{-1} at 415 nm and $\epsilon(P_-) = 4.9 \times 10^4$ M^{-1} cm^{-1} at 490

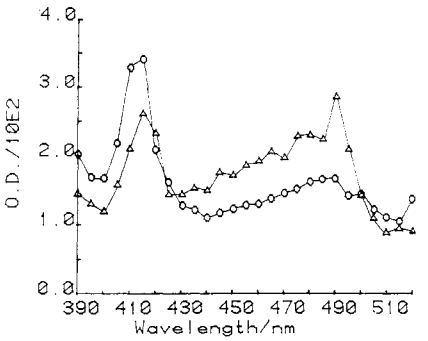

Figure 4. Transient absorption spectra of pyrene and DMA in PA-18K_2 (○) and in SDS (△): [pyrene] = 6×10^{-5} M, [DMA] = 3 mM.

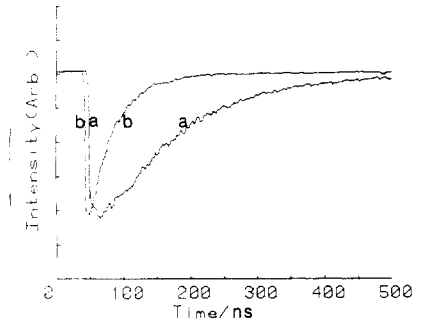

Figure 5. Time-dependent profiles of exciplex fluorescence of pyrene–DMA observed at 470 nm in PA-18K_2 (a) and in SDS (b) (system as same as Figure 4).

nm, respectively. Then the relative ratio of ϕ_T to ϕ_- is measured as 3.3 in PA-18K_2 and 1.3 in SDS micellar system.

For the pyrene–DMA exciplex, the suggested mechanism[19] of the photolysis of pyrene and DMA is

$$P_s^* + D \rightarrow (P^*\cdots D)_s \xrightarrow{k_{ip}} p^{\bullet-} + p^{\bullet+} \quad \text{ionic photodissociation}$$

$$P_s^* + D \rightarrow (P^*\cdots D)_s \xrightarrow{k_{isc}} (P^*\cdots D)_T \quad \text{intersystem crossing}$$

$$P_s^* + D \rightarrow (P^*\cdots D)_s \xrightarrow{k_f} P + D \quad \text{fluorescence emission}$$

$$P_s^* + D \rightarrow (P^*\cdots D)_s \xrightarrow{k_{nr}} P + D \quad \text{nonradiative process}$$

Mataga and co-workers[19] have indicated that the yields of pyrene anion are related to the dielectric constants of the solvent. In polar solvents, the ionic photodissociation process, k_{ip}, is dominant amongst the decay process of exciplex $(P^*\cdots D)_s$, and the relative ratio of ϕ_T to ϕ_- is low. On the contrary, in nonpolar solvents, k_{ip} is greatly depressed, the intersystem crossing process gives the exciplex which then dissociates to P_T^*, and a higher yield of ϕ_T relative to ϕ_- is obtained. The higher ratio of ϕ_T to ϕ_- observed in PA-18K_2 again indicates that the environment of the pyrene–DMA pair in PA-18K_2 is less polar than that in SDS.

The time-dependent profiles of exciplex fluorescence of pyrene–DMA monitored at 470 nm in PA-18K_2 are shown in Figure 5; the decay in SDS is also given in Figure 5 for sake of comparison. The data indicate that the pyrene–DMA exciplex in SDS micellar solution is formed rapidly in several nanoseconds and then decays with a lifetime of 43 ns. However, the intensity of the exciplex in PA-18K_2 grows to a maximum over 40 ns, followed by a decay over

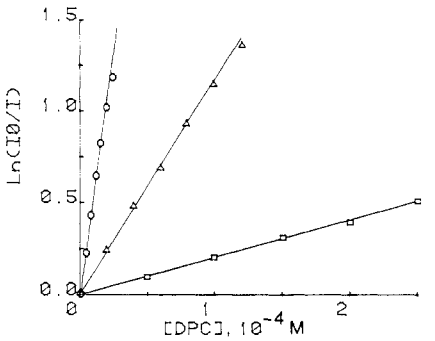

Figure 6. Plots of ln (I_0/I) of C_4PN^+ fluorescence vs. the concentration of quencher, DPC, in PA-18K_2 of various concentrations: 2×10^{-5} M (○), 1×10^{-4} M (△), and 5×10^{-4} (□); [C_4PN^+] = 4×10^{-6} M.

121 ns. The latter behavior mirrors that observed in hexane (130 ns).[20] A slower formation of exciplex can be attributed to the restriction of movement of pyrene and DMA molecules by the PA-18K_2, while the longer lifetime of the exciplex originates from the nonpolar environment of the guest molecules in PA-18K_2.

Aggregation Number of Monomer Units in PA-18K_2 Micelle. Quenching experiments of C_4PN^+ by DPC were undertaken in aqueous solutions of PA-18K_2. The steady-state quenching data do not fit simple Stern–Volmer kinetics, i.e., I_0/I vs. [Q] is not linear, but fit quenching kinetics:[21,22]

$$\ln (I_0/I) = \frac{[Q]}{[\text{micelle}]} \tag{1}$$

The quenching data were obtained at PA-18K_2 concentrations of 2×10^{-5}, 1×10^{-4}, and 5×10^{-4} M, corresponding to the concentrations of monomer units $[PA\text{-}18K_2]_M$ of 4.5×10^{-4}, 2.25×10^{-3}, and 1.13×10^{-2} M, respectively. The plots of ln (I_0/I) vs. [Q] are shown in Figure 6. The slope of this curve is 1/[micelle], and the concentration of monomer units in PA-18K_2 is known. The mean aggregation number, $\bar{N}$, then can be estimated as 24 ± 2 via

$$\bar{N} = \frac{[PA\text{-}18K_2]_M - CMC}{[\text{micelle}]} \tag{2}$$

where the CMC for the polymer is taken as zero, as PA-18K_2 does not possess free monomer units. The same method gave an aggregation number of SDS micelle as 64, which is in good agreement with the literature value of 62.[23]

Pulsed studies of the above quenching process confirm the Poisson distribution of DPC molecules among the polymer micelles. The time-dependent quenching data fit the equation[24]

$$I = I_0 \exp\{(-k_0 t) - \bar{n}[1 - \exp(-k_q t)]\} \tag{3}$$

(standard deviation $\leq 5 \times 10^{-4}$), where $\bar{n}$ denotes the average number of DPC molecules solubilized in each polymer micelle and k_0 and k_q are the first-order rate constants for the decay of pyrene in the absence and in the presence of quencher, respectively. The values of $\bar{n}$, k_0, and k_q are given by computer fitting via eq 3.

The Poisson kinetic quenching parameters, k_0 and k_q, as well as calculated $\bar{N}$ and $\bar{W}_{micelle}$ are presented in Table III. k_q in SDS micelle is twice as fast as that in PA-18K_2, indicating the greater restriction to movement in the polymer micelle. The aggregation number of monomer units in the polymer micelle, $\bar{N}$, calculated from $\bar{n}$, [Q], and $[PA\text{-}18K_2]_M$ according to eq 4 and 2, is in good agreement

$$\bar{n} = \frac{[Q]}{[\text{micelle}]} \tag{4}$$

Table III
Kinetic Parameters in Quenching of C_4PN^+ Fluorescence[a] by DPC[b] in PA-18K$_2$ and in SDS Micellar Solutions

parameters	PA-18K$_2$	SDS
k_o, s^{-1}	4.4×10^6	4.9×10^6
k_q, s^{-1}	1.5×10^7	3.7×10^7
$\bar{N}$	25	64
$\bar{W}_{micelle}$	1.0×10^4	1.8×10^4

[a] $[C_4PN^+] = 4 \times 10^{-6}$ M. [b] DPC = 1-dodecylpyridinium chloride.

with that obtained from the steady-state studies quenching data. The polymer micelle weight, $\bar{W}_{micelle}$, then was obtained by eq 5 where M_m is the molecular weight of monomer. The polymer micelle weight calculated from Poisson quenching kinetics (M_m = 428) corresponds to the polymer molecular weight measured by HPLC (see the Experimental Section). This indicates that one PA-18K$_2$ polymer molecule of molecular weight 1×10^4 forms one polymer micelle. In the case of SDS, the results from pulsed studies and steady-state studies are identical.

$$\bar{W}_{micelle} = \bar{N}M_m \quad (5)$$

The above experiment results show that Poisson quenching kinetics, which are successful in measuring mean aggregation numbers in simple micellar systems,[21-24] can also be used to investigate the polymer micelle.

Polymeric Micelle–Pyrene Equilibrium Association Constants. The partitioning of a fluorescent probe pyrene (Py) between an aqueous phase and a polymeric micelle (M) may be described as equilibrium 6, assuming that

$$Py + M \rightleftharpoons Py\text{–}M \quad (6)$$

$$k_{eq} = \frac{[Py\text{–}M]}{[Py][M]} = \frac{[Py\text{–}M]}{[Py][PA\text{-}18K_2]} \quad (7)$$

pyrene and PA-18K$_2$ polymer form a 1:1 complex. In eq 6 and 7, [Py] denotes the concentration of pyrene in water, [Py–M] is that in PA-18K$_2$ polymer, and [M] represents the concentration of polymeric micelle which is identical with the PA-18K$_2$ polymer chain concentration, [PA-18K$_2$]. According to the above Poisson quenching kinetic results, viz., one PA-18K$_2$ polymer chain of molecular weight 1×10^4 forms one polymer micelle. Therefore, it can be assumed that two types of fluorescent species, Py and Py–M, are present in aqueous solutions of PA-18K$_2$, leading to a nonlinear exponential decay of pyrene fluorescence. The decay data of pyrene fluorescence at the lower concentration range of PA-18K$_2$, 2×10^{-6}–2×10^{-5} M, do fit a double exponential by the expression

$$I(t) = I(0)[\alpha \exp(-k_1 t) + (1 - \alpha) \exp(-k_2 t)] \quad (8)$$

where k_1 and k_2 are the decay rate constants of pyrene fluorescence in aqueous phase and in PA-18K$_2$, respectively, and α indicates the fraction that decays in water.[11b,c] The values of α as well as k_1 and k_2 were obtained by computer fitting. At concentrations of PA-18K$_2$ above 2×10^{-5} M or below 1×10^{-6} M, α values are either too small or too big to measure accurately, and decays of pyrene fluorescence approaches single-exponential first-order kinetics.

From the definition of α, the following relationship can be derived:[25a]

$$(1 - \alpha)/\alpha = ([Py\text{–}M]/[Py])(\epsilon_{Py\text{–}M}/\epsilon_{Py})(\phi_{Py\text{–}M}/\phi_{Py}) \quad (9)$$

where the ratios of the absorption coefficients of pyrene at the excitation wavelength in water and in PA-18K$_2$, $\epsilon_{Py\text{–}M}/\epsilon_{Py}$, are assumed to be identical[25b] and the ratio of quantum yield, $\phi_{Py\text{–}M}/\phi_{Py}$, was estimated as 2.0, the ratio of natural decay rates of pyrene, $k^0_{Py}/k^0_{Py\text{–}M}$. Then, eq 10 can be constructed from (7) and (9).

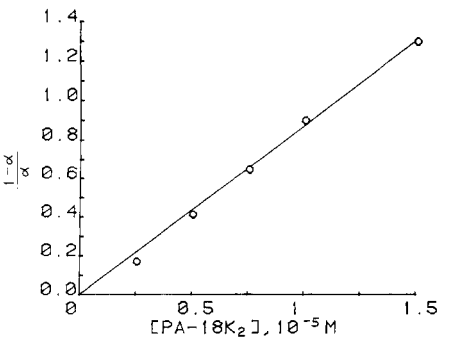

Figure 7. Plot of $(1 - \alpha)/\alpha$ vs. the concentration of PA-18K$_2$.

$$\frac{1 - \alpha}{\alpha} = 2.0 k_{eq}[PA\text{-}18K_2] \quad (10)$$

Hashimoto estimated the equilibrium association constants, K_{eq}, of pyrene–β-cyclodextrin by a similar equation,[25a] where he used quenchers copper(II) and thallium(I) in order to enhance the differences between k_1 and k_2 in double-exponential kinetics. However, in the present study, the cationic quenchers electrostically bind to high ionized PA-18K$_2$ polymer micelle at pH 8, leading static quenching kinetics which will change the entire kinetic model. Therefore, nonquencher data are directly applied.

Figure 7 shows the plot of $(1 - \alpha)/\alpha$ vs. the concentration of PA-18K$_2$. α values were determined from pyrene fluorescence. The linear plot confirms the starting assumptions. The K_{eq} value, 4.5×10^4 M^{-1}, estimated from the slope of this plot and eq 10 was one-thirtieth that previously determined in SDS micelle.[26] The data indicates a more rigid structure for polymeric micelle compared to normal micelles, which leads to a smaller solubility of guest molecules in PA-18K$_2$ compared to simple micelle.

Conclusion

The polymer micelle, PA-18K$_2$, provides an interesting extension of simple micelles, both with regard to solubilizing power as well as effects of polymer chain on photoreactions induced in the system. Photostudies provide further direct evidence for the formation of compact coil conformations in PA-18K$_2$ over the entire pH range, quite unlike PMA which only forms compact coils in strongly acidic solutions. Data on the degree of fluorescence polarization and the rate constants of photoreactions both show that the guest molecules in polymer micelles experience a much more rigid environment than in SDS micelles. The polymer main chain places a steric restrictive effect and/or electrostatic effect on movement of guest reactants. These studies also show that the interior of a PA-18K$_2$ polymer micelle is more hydrophobic than SDS but is similar to that in SCS. In further studies we intend to use the higher molecular weights of PA-18K$_2$ in order to investigate the effect of polymer molecular weight on the aggregation of intramolecular polymeric micelles.

Acknowledgment. We thank the National Science Foundation for the support of this work via Grant CHE-01226-02. We are also grateful to the Chevron/Gulf Co. for kindly providing the free polymer sample of PA-18.

Registry No. DMA, 30918-95-7; DPC, 104-74-5; PA-18K$_2$, 108919-60-4; C_4PN^+, 108919-58-0; $C_{11}PN^+$, 103692-03-1; PyC_3CO_2H, 3443-45-6; $PyCaCO_2H$, 64701-47-9; $PySO_3Na$, 59323-54-5; Py, 129-00-0; Tl^+, 22537-56-0; O_2, 7782-44-7; H_3CNO_2, 75-52-5; I^-, 20461-54-5.

References and Notes

(1) Thomas, J. K. *The Chemistry of Excitation at Interfaces*; ACS Monograph Series 181; American Chemical Society: Washington, DC, 1984.
(2) Fendler, J. *Membrane Mimetic Chemistry*; Academic: New York, 1983.
(3) Turro, N. J.; Grätzel, M.; Braun, A. M. *Angew. Chem., Int. Ed. Engl.* **1980**, *19*, 675.
(4) Setton, R. In *Chemical Reactions in Organic and Inorganic Constrained Systems*; Nato ASI Series C; D. Reidel: New York, 1985; Vol. 165.
(5) Strauss, U. P.; Gersheld, N. L. *J. Phys. Chem.* **1954**, *58*, 747. Strauss, U. P.; Gersheld, N. L.; Crook, E. H. *Ibid.* **1956**, *60*, 577; *Polymer Prepr.* **1986**, *27*(1) 425.
(6) (a) Wang, K. H.; Kimura, K.; Smid, J. *J. Polym. Chem.* **1983**, *21*(2) 579. (b) Roland, B.; Kimura, K.; Smid, J. *J. Colloid Interf. Sci.* **1984**, *97*(2), 392. (c) Roland, B.; Smid, J. *J. Am. Chem. Soc.* **1983**, *105*, 5269.
(7) Geacintov, N. E.; Prusic, T.; Khosrofian, J. *J. Am. Chem. Soc.* **1976**, *98*, 6444 and references therein.
(8) Strauss, U. P. In *Microdomains in Polymer Solutions*; Dubin, P., Ed.; Plenum: New York, 1985; pp 1–12.
(9) Sugai, S.; Nitta, K.; Ohno, N. In *Microdomains in Polymer Solutions*; Dubin, P., Ed.; Plenum: New York, 1985; pp 13–32.
(10) Nakahira, T.; Grätzel, M. *Macromol. Chem. Rapid Commun.* **1985**, *6*, 341.
(11) (a) Chu, D. Y.; Thomas, J. K. *Macromolecules* **1984**, *17*, 2142. (b) Chu, D. Y.; Thomas, J. K. *J. Phys. Chem.* **1985**, *89*, 4065. (c) Chu, D. Y.; Thomas, J. K. *J. Am. Chem. Soc.* **1986**, *108*, 6270.
(12) (a) Shinitzky, M.; Dianoux, A. C.; Gitler, C.; Weber, G. *Biochemistry* **1971**, *10*, 2106. (b) Grätzel, M.; Thomas, J. K. *J. Am. Chem. Soc.* **1973**, *95*, 6885. (c) Azumi, T.; McGlynn, S. P. *J. Chem. Phys.* **1962**, *37*, 2413.
(13) Hashimoto, S.; Thomas, J. K. *J. Phys. Chem.* **1985**, *89*, 2771.
(14) Kalyanasundaram, K.; Thomas, J. K. *J. Am. Chem. Soc.* **1977**, *99*, 2039.
(15) Nakamura, T.; Thomas, J. K. *Langmuir* **1985**, *1*, 568.
(16) Chen, T.; Tomas, J. K. *J. Polym. Sci., A-1* **1979**, *17*, 1103.
(17) Katusin-Razem, B.; Wong, M.; Thomas, J. K. *J. Am. Chem. Soc.* **1978**, *100*, 1679.
(18) (a) Heinzelmann, W.; Labhart, H. *Chem. Phys. Lett.* **1969**, *4*, 20. (b) Jagur-Grodzinski, J.; Feld, M.; Yang, S. L.; Szwarc, M. *J. Phys. Chem.* **1965**, *69*, 628. (c) Schomburg, H.; Steark, H.; Weller, A. *Chem. Phys. Lett.* **1973**, *21*, 433.
(19) (a) Birks, J. B. *Photophysics of Aromatic Molecules*; Wiley-InterScience: New York, 1970; p 429. (b) Mataga, N.; Okada, T.; Yamamoto, N. *Bull. Chem. Soc. Jpn.* **1966**, *39*, 2562; *Chem. Phys. Lett.* **1967**, *1*, 119.
(20) Reference 19(a), p 479.
(21) Turro, N. J.; Yekta, L. A. *J. Am. Chem. Soc.* **1958**, *100*, 5951.
(22) Reference 1, p 172.
(23) Fendler, J. H.; Fendler, E. J. *Catalyst in Micellar and Macromolecular Systems*; Academic: New York, 1975.
(24) (a) Tachiya, M. *Chem. Phys. Lett.* **1975**, *33*, 289; *J. Chem. Phys.* **1982**, *76*, 340. (b) Atik, S. S.; Singer, L. A. *Chem. Phys. Lett.* **1978**, *59*, 519.
(25) (a) Hashimoto, S.; Thomas, J. K. *J. Am. Chem. Soc.* **1985**, *107*, 4655. (b) Nakajima, A. *Bull. Chem. Soc. Jpn.* **1984**, *57*, 1143 and references therein.
(26) Almgren, M.; Grieser, F.; Thomas, J. K. *J. Am. Chem. Soc.* **1979**, *101*, 279.

Regime Transitions in Fractions of *cis*-Polyisoprene

P. J. Phillips* and N. Vatansever

Department of Materials Science and Engineering, The University of Tennessee, Knoxville, Tennessee 37996-2200.

Received October 15, 1986

ABSTRACT: Relatively narrow fractions of *cis*-polyisoprene have been prepared from hevea rubber by nonsolvent precipitation. Following molecular weight characterization by intrinsic viscosity and gel permeation chromatography, crystallization studies were conducted using osmium tetraoxide staining followed by transmission electron microscopy. Kinetic curves are typically bell shaped, the rate of crystal growth decreasing as molecular weight is increased. Secondary nucleation analyses show that the regime II–regime III transition occurs for fractions of lower molecular weight but that generally only regime III growth can be easily observed for molecular weights of 897 000 and above. Narrow fractions show a ratio of slopes for regime III to regime II close to 2.0 as predicted by theory whereas unfractionated systems give lower values (e.g., 1.65 for *cis*-polyisoprene from hevea rubber). Detailed studies of a fraction of molecular weight 313 000 show an extremely distorted bell-shaped crystallization curve. Kinetic analyses of the data demonstrate clearly the presence of all three crystallization regimes for the first time in any polymer. Morphological studies confirm the presence of a regime I–regime II transition. A major increase in branching occurs at temperatures just below that transition, as in polyethylene. The regime I region is characterized by molecular weight fractionation manifest by the concurrent presence of both axialites and single crystals with grossly different growth rates. This experimentation provides the first clear evidence for regime theory as currently developed.

Introduction

Recent major advances in our understanding of quiescent crystallization in polymers have resulted from the discovery of different regimes of nucleation. Prior to this advance it was generally assumed that nucleation on a crystal surface was always the rate-controlling event in lamellar growth.[1] The suggestion of a transition as a function of temperature and molecular weight from a situation where the nucleation rate was considerably slower than the rate of lateral spreading (regime I) to a condition where the two rates are comparable (regime II) was made by Lauritzen and Hoffman[2] in 1973. Experimental confirmation of this transition in narrow fractions of linear polyethylene followed shortly thereafter.[3] It has now been demonstrated[4] that the effect can be observed in bulk crystallization of the unfractionated polymer and that the pressure dependence of the transition follows that of the equilibrium melting point. Only one other polymer is believed to show a similar regime transition[5] although poly(ϵ-caprolactone) shows such an effect with time presumably due to a less narrow molecular weight distribution than polyethylene.[6]

The prediction of a second transition at even lower supercoolings, from regime II to regime III, was first made by Phillips in 1979[7] and an appropriate theory was formulated by Hoffman in 1983.[8] Such a transition is now believed to occur in several polymers including cis-polyisoprene,[9,10] polypropylene,[11] and poly(phenylene sulfide).[12] Studies of the regime II–regime III transition analogous to those of the regime I–regime II transition in polyethylene as a function of molecular weight and temperature

* To whom all correspondence should be addressed.

0024-9297/87/2220-2138$01.50/0